Boron Chemistry, **1996**, p. 3; b) K. A. Solutsev, A. M. Mebel, N. A. Votinova, N. T. Kuznetsov, O. P. Charkin, *Sov. J. Coord. Chem. (Engl. Trans.)* **1992**, *18*, 296; *Koord. Khim.* **1992**, *18*, 340.

[20] The recording and calculation (NICS) of the ^{27}Al NMR spectra are subject of ongoing investigations.

[21] The species $Al_2Br_4 \cdot 2D$ has already been structurally characterized with D = OMePh as stabilizing donor.[26]

[22] RIDFT, BP86-functional, SV(P)-basis, Turbomole program package; O. Treutler, R. Ahlrichs, *J. Chem. Phys.* **1995**, *102*, 346; K. Eichkorn, O. Treutler, H. Ohm, M. Häser, R. Ahlrichs, *Chem. Phys. Lett.* **1995**, *242*, 652. Quantum chemical calculations for AlX compounds have shown that the halogen (Cl or Br) and the donor (H_2O or THF) do not have a significant influence on the values considered here of the investigated Al species.[27]

[23] The calculation shows that during the formation of **1** about 99 % of the disproportion energy is liberated. Owing to the mathematical approximation and the connection between the calculated data and the experimentally determined sublimation energy of aluminum (accuracy: ± 5 kJ mol^{-1}), exact quantifications are difficult, that is these results only serve as preliminary information on the energetic situation.

[24] A. Ecker, E. Weckert, H. Schnöckel, *Nature* **1997**, *387*, 379.

[25] E. J. M. Hamilton, G. T. Jordan IV, E. A. Meyers, S. G. Shore, *Inorg. Chem.* **1996**, *35*, 5335.

[26] M. Mocker, C. Robl, H. Schnöckel, *Angew. Chem.* **1994**, *106*, 946–948; *Angew. Chem. Int. Ed. Engl.* **1994**, *33*, 862.

[27] A. Ecker, E. Baum, M. A. Friesen, M. A. Junker, C. Üffing, R. Köppe, H.Schnöckel, *Z. Anorg. Allg. Chem.* **1998**, *624*, 513–516.

[28] W. Kabsch, *J. Appl. Crystallogr.* **1993**, *26*, 795–800.

Convergence of Catalytic Antibody and Terpene Cyclase Mechanisms: Polyene Cyclization Directed by Carbocation–π Interactions**

Chiana M. Paschall, Jens Hasserodt, Terri Jones, Richard A. Lerner, Kim D. Janda, and David W. Christianson*

Carbocation cyclization cascades catalyzed by terpenoid cyclases rank among the most important and the most complex carbon–carbon bond forming reactions in chemistry and biology.[1, 2] For example, consider the pathway of cholesterol biosynthesis in which the open-chain polyene squalene oxide is cyclized to yield the tetracyclic product lanosterol in a single chemical reaction catalyzed by lanosterol synthase (Scheme 1 A).[2] More than one third of the carbon atoms in the triterpene substrate undergo changes in bonding and/or hybridization during the cyclization cascade to yield a product containing seven precisely formed stereocenters. Remarkably, only 1 out of a possible 128 product stereoisomers is generated, so one key role of the cyclase is to mediate the structural and stereochemical precision of the cyclization reaction. Such precision is the hallmark of most terpenoid cyclases, which are responsible for the biosynthesis of myriad natural products in all forms of life.

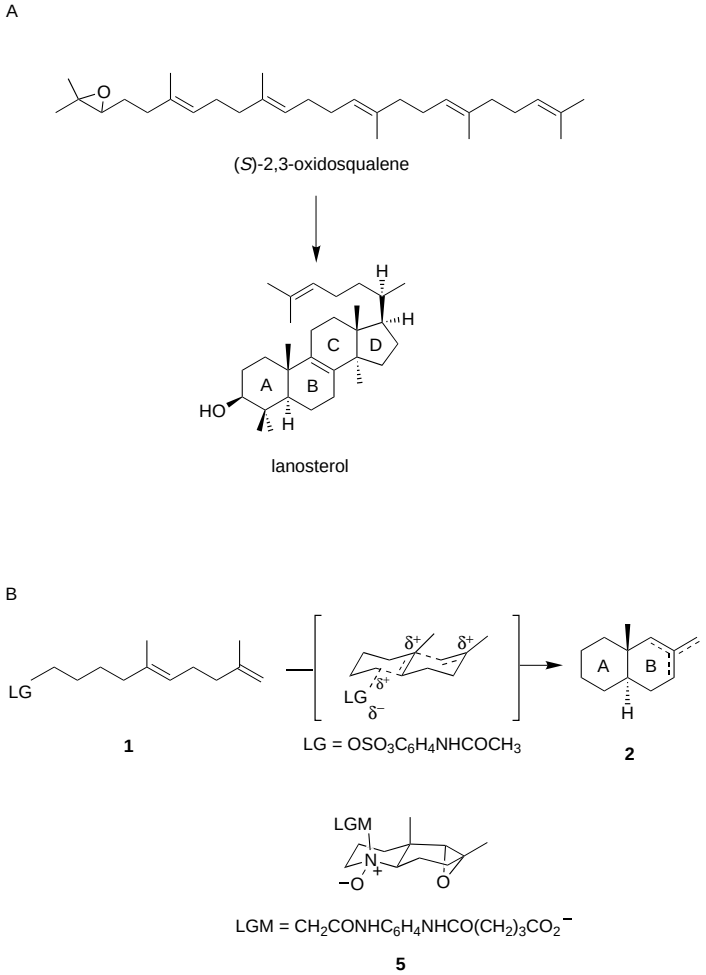

Scheme 1. A) Cyclization catalyzed by lanosterol synthase. Lanosterol rings are labeled according to the standard steroid nomenclature. B) Polyene cyclization catalyzed by antibody HA5-19A4 yields a *trans*-decalin skeleton analogous to the lanosterol A and B rings. LGM = leaving group mimic plus carrier protein linker. For further information see the text.

Recent X-ray crystal structure determinations of terpenoid cyclases suggest an independent evolution of two classes of cyclases, yet members of each class exhibit convergent structural features important for catalysis.[3] The active site cavities of each are nested deep within α-helical superstructures, where numerous hydrophobic residues help to sequester the linear polyene substrate from solvent and form

[*] Prof. Dr. D. W. Christianson, C. M. Paschall
Roy and Diana Vagelos Laboratories
Department of Chemistry, University of Pennsylvania
Philadelphia, PA 19104-6323 (USA)
Fax: (+1) 215-573-2201
E-mail: chris@xtal.chem.upenn.edu
Prof. Dr. J. Hasserodt, T. Jones, Prof. Dr. R. A. Lerner, Prof. Dr. K. D. Janda
Department of Chemistry and
The Skaggs Institute for Chemical Biology
The Scripps Research Institute
10550 N. Torrey Pines Road
La Jolla, CA 92037 (USA)

[**] This work was supported by NIH grants GM56838 (D.W.C.) and GM43858 (K.D.J.) and the Skaggs Institute for Chemical Biology. C.M.P is supported by a Fontaine Fellowship from the University of Pennsylvania and an NSF Minority Fellowship Award. We thank Lisa Kerwin for preparation of the Fab. Additionally, we thank J. D. Cox, C. A. Lesburg, T. Stams, and R. Stanfield for helpful discussions during the course of this investigation.

  1433-7851/99/3812-1743 $ 17.50+.50/0

a template to enforce the unique substrate conformation and stereochemistry required for cyclization. Furthermore, each active-site cavity contains aromatic residues that are poised to stabilize any carbocation cyclization intermediates (and their associated transition states) through cation–π interactions.[4] Additional polar residues in each active site likely participate in electrostatic stabilization and govern the regiochemistry of the deprotonation and/or protonation steps required in the cyclization mechanism. Structural relationships within each class of terpenoid cyclases indicate divergence from the primordial class I and II cyclase ancestors early in the evolution of terpenoid biosynthetic pathways.[3] The facile evolution of the ancestral terpenoid cyclase maximizes the potential product diversity that arises from a minimal polyene substrate pool.

Catalytic antibody technology[5] provides an alternative approach that can be exploited to maximize the diversity of cyclization products starting from a polyene substrate. Importantly, catalytic antibody cyclases are not limited to a handful of naturally occurring polyene substrates, so their potential product diversity is even greater than that of naturally occurring terpenoid cyclases. Several antibodies have been generated to date that catalyze cationic cyclization reactions,[6] and one in particular catalyzes a terpenoid-like cyclization reaction:[7] antibody HA5-19A4 catalyzes the tandem cationic cyclization of polyene substrate **1** to form the bridge-methylated *trans*-decalin skeleton **2** (Scheme 1). This bicyclic product is analogous to that formed by the steroid A and B rings of lanosterol in the cyclization of squalene oxide (Scheme 1). The rate of the antibody-catalyzed reaction $k_{cat} = 0.021\ min^{-1}$ [7] means that the catalytic turnover approaches that measured for many terpenoid cyclases; the absolute rate enhancement over the uncatalyzed reaction rate is immeasurably large, as is typical for a terpenoid cyclase. Antibody HA5-19A4 was raised against hapten **5**, which partially mimics the productive chair–chair conformation required for polyene cyclization to the *trans*-decalin (Scheme 1). As part of a "bait-and-switch" strategy[6–8] the hapten design also incorporated the *N*-oxide moiety, which was intended to elicit functional groups in the antibody combining site that would facilitate departure of the leaving group.

We have determined the X-ray crystal structure of the Fab fragment of the catalytic antibody HA5-19A4 complexed with hapten **5**. The structure of the complex shows that the bicyclic hapten is buried deep within the antibody combining site, and intermolecular interactions provide critical structural inferences on the mechanism of polyene cyclization (Figure 1). The antibody combining site is hydrophobic in nature with numerous aromatic residues in close proximity to the hapten and its linker. Together with the aliphatic residues in the antibody combining site the aromatic residues provide for a highly complementary fit with the hapten. In accord with theories underlying hapten design[7] the catalytic antibody serves as a precise template for catalysis: the active site has a specific contour that binds the polyene substrate in a productive chair–chair conformation, poised to proceed along the reaction coordinate of carbon–carbon bond formation once formation of the carbocation is triggered (Figure 2). This lowers the conformational entropic barrier to catalysis[9] and accelerates the polyene cyclization reaction.

Hydrogen-bond interactions in the Fab–**5** complex provide the first confirmation of the "bait-and-switch" strategy for hapten design. This result highlights a subtle, yet important, point: not only can the structure of the hapten incorporate features anticipated in a catalytic transition state, but it can also include additional functional groups that will elicit complementary functional groups in the antibody combining

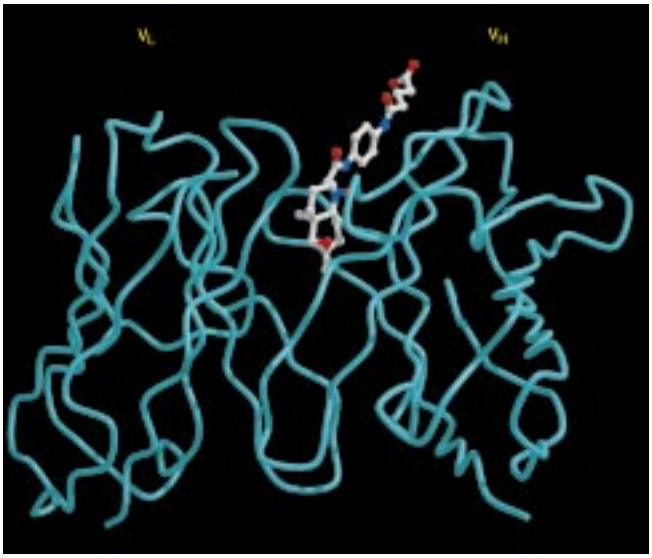

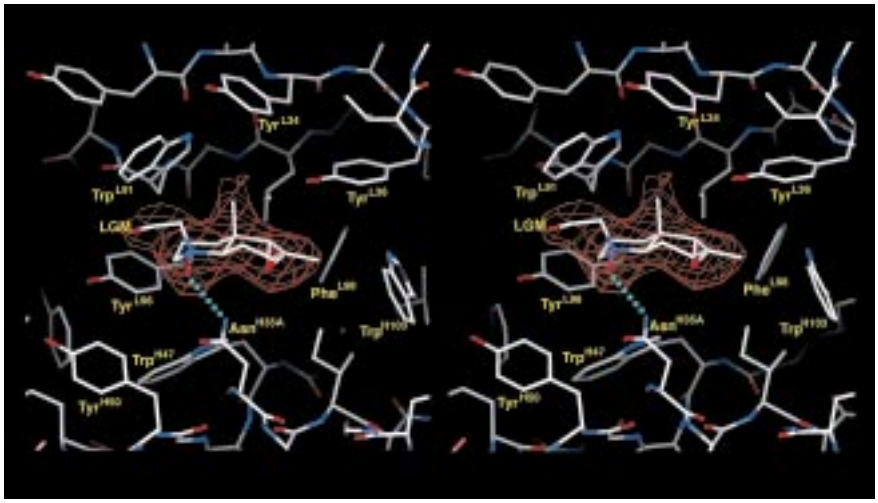

Figure 1. Top: Cα backbone of the variable region of the Fab, showing the location of the bound hapten.[21] Bottom: Stereoview of the omit electron density map of the hapten (contoured at 3.4σ); numerous aromatic residues surround the hapten to form a highly complementary contour. For clarity only a portion of the leaving group mimic (LGM) is shown. A hydrogen bond between the oxygen atom of the *N*-oxide moiety and Asn^{H35A} (cyan dotted line) reflects the likely role of this residue in triggering the departure of the leaving group in catalysis.

  1433-7851/99/3812-1744 $ 17.50+.50/0

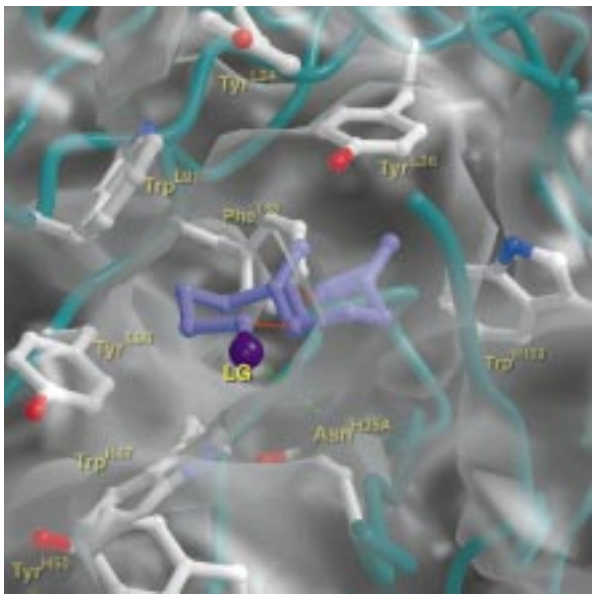

Figure 2. Model of polyene substrate **1** binding with the productive chair–chair conformation (lavender), based on the structure of the Fab-**5** complex; the reaction coordinates of the carbon–carbon bond formation are indicated by red dotted lines.[21] Selected aromatic residues which contribute to the active site template for substrate binding are indicated. Additionally, Asn^{H35A}, which is believed to help trigger departure of the leaving group (LG) by hydrogen bonding with the sulfonate group of the substrate, is indicated (green dashed line; for clarity the leaving group is designated as a simple purple sphere).

site to participate in a specific chemical step of catalysis. The side chain of Asn^{H35A} donates a hydrogen bond to the negatively charged oxygen atom of the *N*-oxide moiety, and the positively charged nitrogen atom of the *N*-oxide moiety (which is isosteric with the substrate C1 atom) interacts with the π-electron clouds of Trp^{L91} and Tyr^{L96}, and to a lesser extent Tyr^{H50} (Figure 3A). Therefore, the initial formation of the carbocation is triggered by at least one hydrogen-bond interaction with the sulfonate leaving group and the electrostatic stabilization of the developing positive charge on C1 by aromatic π-electron clouds. A concerted attack of the C5–C6 π bond avoids any significant formation of an unfavorable primary carbonium ion at C1 and forms the 6-membered A ring of the *trans*-decalin, yielding an intermediate with a favorable tertiary carbonium ion at C5 (Scheme 2).[7] Notably, the π-electron clouds of Tyr^{L36}, Trp^{L91}, and to a lesser extent Tyr^{L34}, are oriented for optimal electrostatic stabilization of the C5 carbocation (Figure 3A). This reaction sequence mimics the first step of the lanosterol synthase mechanism, where formation of the A ring of lanosterol occurs in concert with the opening of the epoxide ring of squalene oxide.[10]

The next step in the catalytic antibody cyclase mechanism is attack of the C5 tertiary carbonium ion intermediate by the C9–C10 π bond to yield the B ring of the *trans*-decalin. The identification of minor side products **3a–c** and **4a,b**, which reflect an incomplete closure of the B ring (Scheme 2),[7] suggests that this step most likely does not occur in concert with formation of the A ring. This is in accord with the cyclization pathway of tetracyclic triterpenes.[2] The closure of the B ring yields an intermediate with a tertiary carbonium ion at C9, and the structure of the Fab–**5** complex reveals that

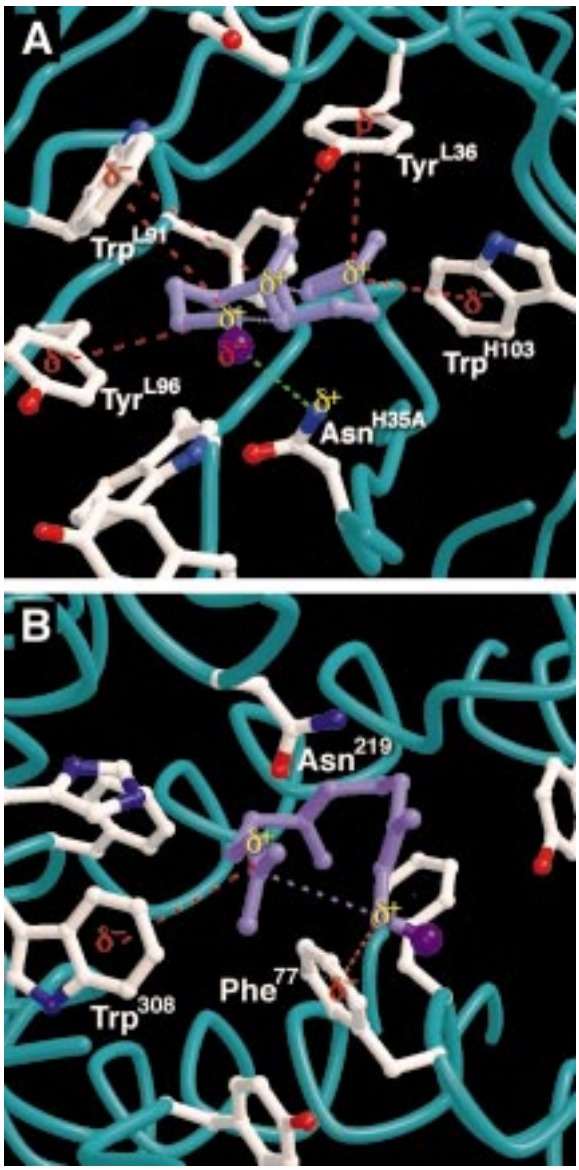

Figure 3. Comparison of A) catalytic antibody HA5-19A4 polyene cyclase and B) pentalenene synthase, which adopt β and α folds, respectively.[21] The reaction coordinates of carbon–carbon bond formation are indicated by lavender dashed lines, and the leaving groups are symbolized by purple spheres, in the models of each enzyme–substrate complex. The departure of the sulfonate leaving group of polyene **1** appears to be triggered in part by a hydrogen bond interaction with Asn^{H35A} in the catalytic antibody (A); metal coordination triggers the departure of the diphosphate leaving group of farnesyl diphosphate in the pentalenene synthase reaction (B). Aromatic residues in each cyclase active site stabilize sites of developing positive charge by electrostatic interactions with aromatic π-electron clouds (red dashed lines). Additional aromatic residues in each active site help define the active site template that enforces the productive binding conformation of the flexible polyene substrate.

the π-electron clouds of Tyr^{L36} and Trp^{H103} are appropriately positioned to stabilize the C9 carbocation (Figure 3A). The fact that the tandem cationic cyclization yields only the *trans*-decalin skeleton **2** indicates that the antibody functions effectively as a chaperone that governs the substrate and intermediate conformations throughout the cyclization cascade to yield a product with exclusive and pre-designed stereochemistry. It is striking that such a broad constellation

  1433-7851/99/3812-1745 $ 17.50+.50/0

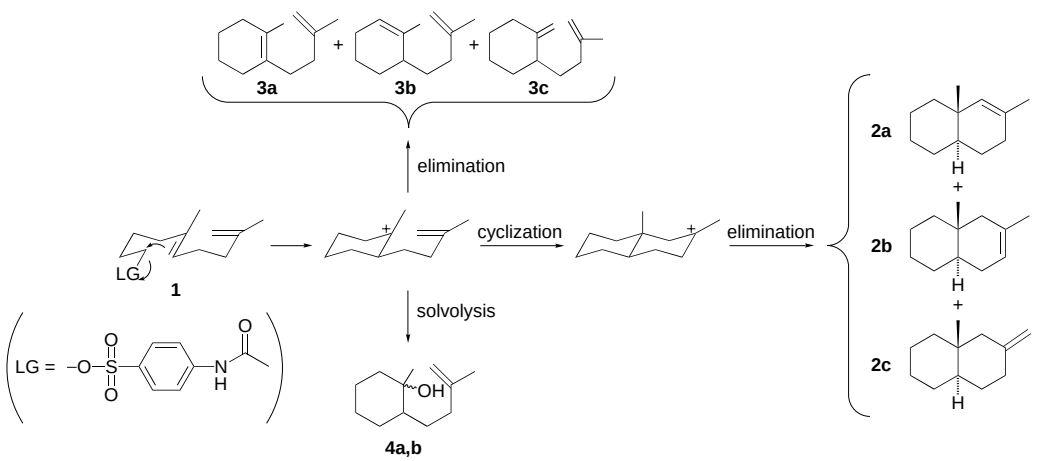

Scheme 2. The mechanism of polyene **1** cyclization catalyzed by antibody HA5-19A4 yields *trans*-decalin regioisomers **2a–c** as the major products. For further information see the text.

of aromatic residues in the active site are appropriately oriented for electrostatic stabilization of developing positive charges at the C1, C5, and C9 atoms of the polyene substrate (Figure 3A). In addition to the aromatic residues that interact directly with these substrate atoms, other aromatic residues line the antibody combining site and possibly contribute some weak, long-range stabilization to the carbocation intermediates. The stabilization of carbocation intermediates by point charges is a strategy known to accelerate polyene cyclization reactions.[11] The stabilization achieved by multiple partial charges should likewise accelerate polyene cyclization reactions, which has been postulated for naturally occurring terpenoid cyclases.[3] Thus, the "unnaturally evolved" antibody cyclase and the naturally evolved terpenoid cyclases have converged to identical strategies for managing and manipulating carbocations in complex cyclization cascades.

A carbocation cyclization cascade is terminated by the addition of a nucleophile (for example, solvent) or elimination of a proton. As part of the "bait-and-switch" hapten design strategy, an oxirane moiety was incorporated into hapten **5** to elicit antibody residues that would facilitate one of two possible termination routes:[12] a) the epoxide oxygen atom could elicit a polar residue to interact with a water molecule that would terminate the C9 carbocation to form an alcoholic product, or b) the 3-membered epoxide ring fixes the B ring of the hapten in a half-chair conformation that could favor proton elimination from the C9 carbocation to form olefinic products with the corresponding half-chair conformations of the B ring. The latter termination route is favored, since olefinic products are predominantly observed.[7] However, the analysis of the olefinic products enabled a mixture of the three possible elimination products to be identified (the closely related regioisomeric *trans*-decalins **2a–c**) present in ratios that reflected their expected thermodynamic stabilities (Scheme 2).[7] The Fab structure reveals that there is no catalytic base to direct the regiochemistry of this final elimination step to yield one exclusive olefin.

The lack of an appropriate basic residue in Fab HA5-19A4 to terminate the carbocation cyclization cascade is reminiscent of the triterpene cyclase squalene–hopene cyclase obtained from *Alicyclobacillus acidocaldarius*, which generates the pentacyclic products hopene (90%, which arises from proton elimination) and hopan-22-ol (10%, which arises from addition of a solvent nucleophile).[13] As with the catalytic antibody cyclase the lack of an appropriate catalytic base in squalene–hopene cyclase results in a mixture of termination products. However, it should be noted that other terpenoid cyclases such as pentalenene synthase and epi-aristolochene synthase do contain active site residues that appear to mediate the regiochemistry of proton transfer steps,[3] so it is likely that such residues can be engineered into any cyclase active site—either by nature or by design.

In closing, it is instructive to compare the general features of convergent evolution in the active sites of the catalytic antibody cyclase HA5-19A4 and pentalenene synthase,[3] a bacterial terpenoid cyclase (Figure 3). Each cyclase exhibits a remarkably different protein fold: the antibody adopts the β fold of an immunoglobulin, and the terpenoid cyclase adopts an α fold. However, each cyclase has a deep, hydrophobic active-site cavity flanked by multiple loops that sequester highly reactive carbocation intermediates from solvent. Additionally, each cyclase contains numerous aromatic residues that, in addition to forming a template to bind the productive conformation of a flexible polyene substrate, stabilize carbocation intermediates by electrostatic interactions with their π-electron clouds. This comprises a highly effective chemical strategy for catalysis:[4] electrostatic stabilization can be achieved without risk of quenching the carbocation and annihilating the protein catalyst if stabilization were achieved with a more polar protein atom. Remarkably, the naturally occurring terpenoid cyclase required millions of years to evolve to this mechanistic strategy, whereas the catalytic antibody required only weeks—the acceleration of convergent evolution highlights the fundamental appeal of catalytic antibody technology. Further exploration and optimization of catalytic antibody HA5-19A4 promises to yield further insight on carbocation cyclization reactions with diverse polyene substrates to yield novel product arrays far beyond the limits of those attainable with naturally occurring terpenoid cyclases.

  1433-7851/99/3812-1746 $ 17.50+.50/0

Experimental Section

Fab HA5-19A4 was prepared by digestion of IgG HA5-19A4 with papain according to a standard protocol (Pierce No. 44885). The IgG was obtained from a standard hybridoma protocol described in the supporting information of Hasserodt and colleagues.[6] For sequence determination the total RNA from 1×10^7 hybridoma cells was prepared with Tri Reagent according to the manufacturer's protocol (Molecular Research Center, Inc., Cincinnati, OH). Reverse transcription and PCR amplification of the light-chain and Fd-fragment sequences were performed as described.[14] The primer 5′-GAYGTNCARCTCGAGGAGTCAGGACCT-3′ was used to amplify the 5′ end of the Fd-fragment sequence. Light-chain and Fd-fragment sequences were digested with *Sac* I/*Xba* I and *Xho* I/*Spe* I, respectively, and ligated into the phagemid vector pComb3H.[15] After electrotransformation into XL1-Blue *E. coli* cells, clones were randomly selected for protein expression induced with isopropyl-β-D-thiogalactopyranoside.[16] Fab specific to HA5-BSA antigen was detected by enzyme-linked immunosorbent assay (ELISA) by using goat anti-mouse $F(ab')_2$ (Pierce) conjugated to alkaline phosphatase as a secondary antibody. Plasmid DNA from ELISA-positive clones was sequenced to determine the light-chain and Fd-fragment sequences.

Crystals of the HA5-19A4 Fab–**5** complex were obtained by equilibrating 5 μL of protein solution (11.4 mg mL^{-1} Fab, 10 mM $CdCl_2$, 10 mM **5**, 50 mM Tris (pH 7.0)) with 5 μL of precipitant buffer (30% polyethylene glycol ($M_r = 6000$), 100 mM 2-[4-(2-hydroxyethyl)-1-piperazinyl]ethanesulphonic acid (HEPES; pH 7.9)) in a hanging drop suspended over a 1 mL reservoir of precipitant buffer at room temperature. Small rectangular plates appeared within three days. These crystals diffracted X-rays with a resolution of 2.7 Å (93.5% complete, $R_{merge} = 0.088$). Crystal dimensions 0.6 mm × 0.1 mm × 0.05 mm, space group $C2$, $a = 101.3$, $b = 70.3$, $c = 69.6$ Å, $\beta = 114.2°$, one molecule in the asymmetric unit. The structure was solved by molecular replacement by using the atomic coordinates[17] of Fab D2.3 to construct a polyalanine probe for rotation and translation function calculations with AmoRe.[18] Refinement and rebuilding of the model were performed with X-PLOR[19] and O;[20] refinement converged smoothly to a final crystallographic R factor of 0.165 ($R_{free} = 0.257$). Two Cd^{2+} binding sites were identified: one between Glu^{L187} and Glu^{L213}, and a second between Asp^{H173} and Glu^{L81} of symmetry-related molecules in the crystal lattice. The final model has excellent stereochemistry with rms deviations from ideal bond lengths and angles of 0.011 Å and 1.7°, respectively. The Ramachandran plot shows that 318, 49, and 3 residues adopt the most favored, additionally allowed, and generously allowed backbone conformations, respectively; only 4 residues adopt disallowed backbone conformations, and these are found in poorly characterized loop regions. Atomic coordinates of the Fab-**5** complex have been deposited in the Brookhaven Protein Data Bank (http://www2.ebi.ac.uk/pdb) with accession code 1CF8.

Received: January 18, 1999 [Z 12925 IE]
German version: *Angew. Chem.* **1999**, *111*, 1859–1864

Keywords: carbocations · catalytic antibodies · cyclases · protein structures · terpenoids

[1] a) L. Ruzicka, *Experientia* **1953**, *9*, 357–367 (one of the six subheadings of this paper is entitled "Biogenesis of Steroids and Terpenic Compounds". Underneath Ruzicka adds a parenthetical comment "(together with A. Eschenmoser and H. Heusser)", along with a citation to Eschenmoser's PhD thesis (ETH Zürich, **1952**)); b) J. W. Cornforth, *Angew. Chem.* **1968**, *80*, 977–985; *Angew. Chem. Int. Ed. Engl.* **1968**, *7*, 903–911; c) W. S. Johnson, *Acc. Chem. Res.* **1968**, *1*, 1–8; d) D. Arigoni, *Pure Appl. Chem.* **1975**, *41*, 219–245; e) D. E. Cane, *Chem. Rev.* **1990**, *90*, 1089–1103; f) D. McCaskill, R. Croteau, *Adv. Biochem. Eng. Biotechnol.* **1997**, *55*, 107–146.

[2] a) I. Abe, M. Rohmer, G. D. Prestwich, *Chem. Rev.* **1993**, *93*, 2189–2206; b) C. Pale-Grosdemange, C. Feil, M. Rohmer, K. Poralla, *Angew. Chem.* **1998**, *110*, 2355–2358; *Angew. Chem. Int. Ed.* **1998**, *37*, 2237–2240.

[3] a) C. A. Lesburg, G. Zhai, D. E. Cane, D. W. Christianson, *Science* **1997**, *277*, 1820–1824; b) C. M. Starks, K. Back, J. Chappell, J. P. Noel, *Science* **1997**, *277*, 1815–1820; c) K. U. Wendt, K. Poralla, G. E. Schulz, *Science* **1997**, *277*, 1811–1815; d) K. U. Wendt, G. E. Schulz, *Structure* **1998**, *6*, 127–133; e) C. A. Lesburg, J. Caruthers, C. M. Paschall, D. W. Christianson, *Curr. Opin. Struct. Biol.* **1998**, *8*, 695–703.

[4] a) S. K. Burley, G. A. Petsko, *Adv. Protein Chem.* **1988**, *39*, 125–189; b) D. A. Dougherty, *Science* **1996**, *271*, 163–168; c) C. Jenson, W. L. Jorgensen, *J. Am. Chem. Soc.* **1997**, *119*, 10846–10854; d) J. C. Ma, D. A. Dougherty, *Chem Rev.* **1997**, *97*, 1303–1324.

[5] a) P. G. Schultz, R. A. Lerner, *Science* **1995**, *269*, 1835–1842; b) T. Li, R. A. Lerner, K. D. Janda, *Acc. Chem. Res.* **1997**, *30*, 115–121.

[6] a) T. Li, K. D. Janda, J. A. Ashley, R. A. Lerner, *Science* **1994**, *264*, 1289–1293; b) T. Li, S. Hilton, K. D. Janda, *J. Am. Chem. Soc.* **1995**, *117*, 3308–3309; c) T. Li, K. D. Janda, R. A. Lerner, *Nature* **1996**, *379*, 326–327; d) J. Hasserodt, K. D. Janda, R. A. Lerner, *J. Am. Chem. Soc.* **1996**, *118*, 11654–11655.

[7] J. Hasserodt, K. D. Janda, R. A. Lerner, *J. Am. Chem. Soc.* **1997**, *119*, 5993–5998.

[8] a) K. D. Janda, M. I. Weinhouse, D. M. Schloeder, R. A. Lerner, S. J. Benkovic, *J. Am. Chem. Soc.* **1990**, *112*, 1274–1275; b) K. D. Janda, M. I. Weinhouse, T. Danon, K. A. Pacelli, D. M. Schloeder, *J. Am. Chem. Soc.* **1991**, *113*, 5427–5434.

[9] M. I. Page, W. P. Jencks, *Proc. Natl. Acad. Sci. USA* **1971**, *68*, 1678–1683.

[10] E. J. Corey, H. Cheng, C. H. Baker, S. P. T. Matsuda, D. Li, X. Song, *J. Am. Chem. Soc.* **1997**, *119*, 1277–1288.

[11] a) W. S. Johnson, S. J. Telfer, S. Cheng, U. Schubert, *J. Am. Chem. Soc.* **1987**, *109*, 2517–2518; b) W. S. Johnson, S. D. Lindell, J. Steele, *J. Am. Chem. Soc.* **1987**, *109*, 5852–5853.

[12] J. Hasserodt, K. D. Janda, *Tetrahedron* **1997**, *53*, 11237–11256.

[13] B. Seckler, K. Poralla, *Biochim. Biophys. Acta* **1986**, *881*, 356–363.

[14] W. D. Huse, L. Sastry, S. A. Iverson, A. S. Kang, M. Alting-Mees, D. R. Burton, S. J. Benkovic, R. A. Lerner, *Science* **1989**, *246*, 1275–1281.

[15] D. Radar, C. F. Barbas, *Curr. Opin. Biotechnol.* **1997**, *8*, 503–508.

[16] C. F. Barbas, A. S. Kang, R. A. Lerner, S. J. Benkovic, *Proc. Natl. Acad. Sci. USA* **1991**, *88*, 7978–7982.

[17] B. Gigant, J.-B. Charbonnier, Z. Eshhar, B. S. Green, M. Knossow, *Proc. Natl. Acad. Sci. USA* **1997**, *94*, 7857–7861.

[18] J. Navaza, *Acta Crystallogr. Sect. A* **1994**, *50*, 157–163.

[19] A. T. Brünger, J. Kuriyan, M. Karplus, *Science* **1987**, *235*, 458–460.

[20] T. A. Jones, J.-Y. Zou, S. W. Cowan, M. Kjeldgaard, *Acta. Crystallogr. Sect. A* **1991**, *47*, 110–119.

[21] Figures were prepared with MOLSCRIPT: P. Kraulis, *J. Appl. Crystallogr.* **1991**, *24*, 946–950; Raster3D: D. J. Bacon, W. F. Anderson, *J. Mol. Graphics* **1988**, *6*, 219–220; E. A. Merritt, M. E. P. Murphy, *Acta Crystallogr. Sect. D* **1994**, *50*, 869–873; BOBSCRIPT: R. M. Esnouf, *J. Mol. Graphics* **1997**, *15*, 132–134; GRASP: B. Honig, A. Nicholls, *Science* **1995**, *268*, 1144–1149.

A Polycationic Metallodendrimer with 24 [Fe(η^5-C_5Me_5)(η^6-*N*-Alkylaniline)]$^+$ Termini That Recognizes Chloride and Bromide Anions

Christine Valério, Ester Alonso, Jaime Ruiz, Jean-Claude Blais, and Didier Astruc*

Dendrimers[1] are the first well-defined, monodisperse synthetic macromolecules that should be able to achieve various supramolecular functions.[2–7] Several applications as, for example, antennas,[3] boxes,[4] and catalysts[5] have already

[*] Prof. D. Astruc, Dr. C. Valério, Dr. E. Alonso, Dr. J. Ruiz
Groupe de Chimie Supramoléculaire des Métaux de Transition
Laboratoire de Chimie Organique et Organométallique (LCOO)
UMR CNRS No. 5802, Université Bordeaux I
351, Cours de la Libération, F-33405 Talence Cédex (France)
Fax: (+33) 5-56-84-66-46
E-mail: d.astruc@lcoo.u-bordeaux.fr
Dr J.-C. Blais
Laboratoire de Chimie Structurale Organique et Biologique
Université Paris VI (France)

Supporting information for this article is available on the WWW under http://www.wiley-vch.de/home/angewandte/ or from the author.

  1433-7851/99/3812-1747 $ 17.50+.50/0